Acta Crystallographica Section D
Biological Crystallography
ISSN 1399-0047

L-*allo*-Threonine aldolase with an H128Y/S292R mutation from *Aeromonas jandaei* DK-39 reveals the structural basis of changes in substrate stereoselectivity

Hui-Min Qin,[a]‡ Fabiana Lica Imai,[a]‡ Takuya Miyakawa,[a] Michihiko Kataoka,[b,c] Nahoko Kitamura,[c] Nobuyuki Urano,[b,c] Koji Mori,[c] Hiroshi Kawabata,[c] Masahiko Okai,[a] Jun Ohtsuka,[a] Feng Hou,[a] Koji Nagata,[a] Sakayu Shimizu[c,d] and Masaru Tanokura[a]*

[a]Department of Applied Biological Chemistry, Graduate School of Agricultural and Life Sciences, The University of Tokyo, 1-1-1 Yayoi, Bunkyo-ku, Tokyo 113-8657, Japan, [b]Division of Applied Life Sciences, Graduate School of Life and Environmental Sciences, Osaka Prefecture University, 1-1 Gakuen-cho, Naka-ku, Sakai 559-8531, Japan, [c]Division of Applied Life Sciences, Graduate School of Agriculture, Kyoto University, Kitashirakawa-Oiwakecho, Sakyo-ku, Kyoto 606-8502, Japan, and [d]Faculty of Bioenvironmental Science, Kyoto Gakuen University, Sogabe-cho, Kameoka 621-8555, Japan

‡ These authors contributed equally to this work.

Correspondence e-mail: amtanok@mail.ecc.u-tokyo.ac.jp

Received 12 November 2013
Accepted 6 April 2014

PDB references: LATA, 3wgb; H128Y/S292R mutant, 3wgc

L-*allo*-Threonine aldolase (LATA), a pyridoxal-5′-phosphate-dependent enzyme from *Aeromonas jandaei* DK-39, stereospecifically catalyzes the reversible interconversion of L-*allo*-threonine to glycine and acetaldehyde. Here, the crystal structures of LATA and its mutant LATA_H128Y/S292R were determined at 2.59 and 2.50 Å resolution, respectively. Their structures implied that conformational changes in the loop consisting of residues Ala123–Pro131, where His128 moved 4.2 Å outwards from the active site on mutation to a tyrosine residue, regulate the substrate specificity for L-*allo*-threonine *versus* L-threonine. Saturation mutagenesis of His128 led to diverse stereoselectivity towards L-*allo*-threonine and L-threonine. Moreover, the H128Y mutant showed the highest activity towards the two substrates, with an 8.4-fold increase towards L-threonine and a 2.0-fold increase towards L-*allo*-threonine compared with the wild-type enzyme. The crystal structures of LATA and its mutant LATA_H128Y/S292R reported here will provide further insights into the regulation of the stereoselectivity of threonine aldolases targeted for the catalysis of L-*allo*-threonine/L-threonine synthesis.

1. Introduction

In recent years, asymmetric synthesis has increasingly been targeted for drug synthesis. The global chiral technology market was worth nearly $5.3 billion in 2011 and will approach $7.2 billion by 2016 (http://bccresearch.wordpress.com/tag/chiral-industry/). Chiral pharmaceuticals can benefit greatly from the selectivity gains associated with enzymatic catalysis (Matsuda *et al.*, 2009; Savile *et al.*, 2010). Compared with chemical reactions, enzymatic syntheses of chiral compounds have the advantages of high enantioselectivity and regioselectivity and of taking place at ambient temperature and atmospheric pressure (Patel, 2008). Threonine aldolases (EC 4.1.2.5) catalyze the aldol reaction of aldehyde and glycine to synthesize threonine or its reverse reaction (Shibata *et al.*, 1996; Vassilev *et al.*, 1995; Liu, Dairi *et al.*, 1997; Liu, Nagata *et al.*, 1997). Threonine is an amino acid with two chiral centres at the α and β C atoms. Therefore, chiral technologies using threonine aldolases require that they can stereoselectively recognize two configurations of threonine. It has been reported that threonine aldolases could also be used for the synthesis of the psychoactive drug L-*threo*-3,4-dihydroxyphenylserine for the treatment of Parkinson's disease (Gwon & Baik, 2010).

Threonine aldolases have been isolated from *Escherichia coli* (Liu, Dairi *et al.*, 1998; di Salvo *et al.*, 2014), *Pseudomonas* (Liu, Ito *et al.*, 1998), *Saccharomyces* (Liu, Nagata *et al.*, 1997), *Candida* (Kumagai *et al.*, 1972) and *Thermotoga* (Kielkopf &

Burley, 2002) as well as from mammals (Karasek & Greenberg, 1957; Roberto *et al.*, 1991; Schirch & Gross, 1968). The threonine aldolases are classified into L-*allo*-threonine aldolases, L-threonine aldolases, low-specificity L-*allo*-threonine/L-threonine aldolases and D-*allo*-threonine/D-threonine aldolases. All four types share a basic reaction mechanism using the cofactor pyridoxal 5′-phosphate (PLP; Kielkopf & Burley, 2002; Matthews *et al.*, 1998). Initially, the PLP cofactor binds to a conserved active-site lysine *via* a Schiff-base linkage. Enzymatic catalysis starts with the threonine substrate forming an external aldimine with PLP, and a retroaldol cleavage of the threonine aldimine then produces acetaldehyde and the PLP–glycine quinonoid complex. The glycine is released along with the protonation of the glycine α C atom, while regenerating the internal Schiff base with the active-site lysine (Supplementary Fig. S1[1]). However, fewer studies on threonine aldolases have been carried out in animal tissues, and in most organisms the route for synthesis of glycine using threonine is the same as the hydroxymethyltransferase (SHMT) pathway (Schirch & Gross, 1968). Many kinds of threonine aldolase from microorganisms exhibit substrate specificity towards threonine and *allo*-threonine, which is not the case with SHMT (Liu, Dairi *et al.*, 1997). Furthermore, catalysis of the glycine synthetic pathway by threonine aldolase has been considered to be an important supplement to that mediated by SHMT (Ogawa *et al.*, 2000).

L-*allo*-Threonine aldolase (LATA) is a member of the aldolase family from *Aeromonas jandaei* DK-39 and consists of 338 amino-acid residues (Liu, Dairi *et al.*, 1997). This enzyme stereospecifically catalyzes the reversible interconversion of L-*allo*-threonine to glycine and acetaldehyde (Supplementary Fig. S2). LATA is considered to achieve this catalysis by a reaction mechanism towards L-*allo*-threonine that is common to all enzymes of this family. Although a few structures of threonine aldolases have been solved, they are restricted to low-specificity L-*allo*-threonine/L-threonine aldolases (Kielkopf & Burley, 2002; di Salvo *et al.*, 2014). Therefore, the structure of LATA will help us to further understand the mechanism of its stereoselectivity towards L-*allo*-threonine.

Here, we report the structures of LATA and its mutant LATA_H128Y/S292R in order to elucidate the structural basis of its stereoselectivity and substrate specificity. Understanding the relationship between the structure and function of LATA could help in regulating its stereoselectivity towards L-*allo*-threonine or L-threonine.

2. Materials and methods

2.1. Random mutagenesis of LATA by error-prone PCR

For error-prone PCR, the plasmid pAJPCR containing the LATA gene (GenBank accession No. D87890), a 5′-primer (5′-GCC**GAATTC**ACCAGGAGGGATGTCATGC-3′) containing the *Eco*RI site (bold) and a 3′-primer (5′-CCG**AAGCTT**CATTCCATGAGATTGTCACG-3′) containing the *Hin*dIII site (bold), prepared as described previously (Liu, Dairi *et al.*, 1997), were used as the template DNA and primers. PCR amplification was carried out in 50 µl of a solution consisting of 10 m*M* Tris–HCl pH 8.3, 1.5 m*M* $MgCl_2$, 50 m*M* KCl, 0.1 m*M* $MnCl_2$, 0.2 m*M* dNTPs, 0.5 µ*M* 5′- and 3′-primers, 2 ng pAJPCR and 2.5 units of *Taq* DNA polymerase (Roche Diagnostics, Basel, Switzerland) at 94°C for 0.5 min, 45°C for 1 min and 72°C for 2 min for a total of 40 cycles. The amplified PCR product was digested with *Eco*RI and *Hin*dIII, and ligated into pUC118 digested with the same restriction enzymes. *E. coli* XL1-Blue MRF′ cells were transformed by the resulting plasmids and then plated onto LB medium containing ampicillin. The *E. coli* transformants were grown aerobically at 37°C in 3 ml LB medium containing 0.1 mg ml^{-1} ampicillin and 0.2 m*M* IPTG. After 24 h of cultivation, the cells were harvested by centrifugation. After suspension in 0.5 ml 100 m*M* potassium phosphate buffer pH 7.5, the cells were disrupted by ultrasonic oscillation at 4°C for 5 min with a Bioruptor (CosmoBio, Tokyo, Japan). The cell debris was removed by centrifugation and the supernatant was used as the cell-free extract.

The threonine aldolase activity of the mutant LATAs was measured essentially according to a previous report (Liu, Dairi *et al.*, 1997). In a 96-well plate, 250 µl of an assay mixture comprising 25 µmol Tris–HCl buffer pH 8.0, 50 nmol NADH, 7.5 U yeast alcohol dehydrogenase (Wako Pure Chemical Industries), 1 µmol L-*allo*-threonine or L-threonine and 10 µl cell-free extract was prepared for each well. The reaction was performed at 303 K and monitored at 340 nm using a SpectraMax 250 (Molecular Devices, Sunnyvale, California, USA).

2.2. Plasmid construction

The DNA sequence encoding full-length LATA was amplified using PCR and was then inserted between the *Eco*RI and *Xho*I sites of the pET-28a(+) vector (Novagen). The LATA protein fused to a hexahistidine (His_6) tag at the N-terminus was expressed. The LATA_H128Y/S292R mutant was selected *via* random mutation using error-prone PCR, showing different stereoselectivity towards L-*allo*-threonine and L-threonine, and the mutant LATA gene was amplified and inserted into pET-28a(+) as described above. S292R mutagenesis and saturation mutagenesis of His128 were carried out by PCR using a QuikChange kit (Stratagene) with the pET-28a(+) plasmid with the LATA sequence insertion as a template. Mutations were confirmed by DNA sequencing.

2.3. Expression and purification

E. coli Rosetta(DE3) cells (Novagen) were transformed with the plasmid and were grown in lysogeny broth (LB) medium containing 100 µg ml^{-1} ampicillin and 34 µg ml^{-1} chloramphenicol at 310 K. When the OD_{600} reached 0.6, isopropyl β-D-1-thiogalactopyranoside (IPTG) was added to a final concentration of 0.5 m*M* and the culture was incubated at 310 K for a further 4 h.

[1] Supporting information has been deposited in the IUCr electronic archive (Reference: MH5119).

After harvesting, the cells were disrupted by sonication in resuspension buffer (50 m*M* Tris–HCl pH 7.5, 100 m*M* NaCl, 1 mg ml^{-1} lysozyme) and the cell debris was removed by centrifugation at 40 000*g*. LATA was trapped on Ni-Sepharose 6 Fast Flow resin (GE Healthcare). After washing, the protein was eluted with 50 m*M* Tris–HCl pH 8.0, 0.5 *M* imidazole, 0.5 *M* NaCl. For preparation of the untagged protein, the N-terminal His_6 tag was removed by adding thrombin (GE Healthcare; 0.5 U per 100 µg of enzyme, 8 h, 298 K) to the eluted fraction. The untagged LATA was further purified on a RESOURCE Q column (GE Healthcare) pre-equilibrated with 20 m*M* Tris–HCl pH 8.0 and was eluted with a linear gradient of 0–1 *M* NaCl. The fractions containing LATA were dialyzed against 20 m*M* Tris–HCl pH 8.0 and then concentrated to 10 mg ml^{-1} for crystallization. The LATA mutants were expressed and purified according to the method described for wild-type LATA.

2.4. Crystallization and data collection

Before crystallization, 250 µ*M* PLP and 20 m*M* glycine were added to the protein solution. LATA was then co-crystallized using the sitting-drop vapour-diffusion method. Crystals were obtained by mixing 1.0 µl protein solution with 1.0 µl reservoir solution consisting of 0.2 *M* ammonium acetate, 0.1 *M* HEPES pH 7.5, 45%(*v*/*v*) MPD at 293 K. LATA_H128Y/S292R was crystallized under the conditions 0.2 *M* ammonium acetate, 0.1 *M* MES pH 6.4, 34%(*v*/*v*) MPD at 293 K.

X-ray diffraction data were collected from the LATA and LATA_H128Y/S292R crystals on the AR-NW12A beamline at the Photon Factory (PF), Tsukuba, Japan. The diffraction data for wild-type LATA were indexed, integrated and scaled with *HKL*-2000 (Otwinowski & Minor, 1997). The diffraction data for LATA_H128Y/S292R were indexed, integrated and scaled with *XDS* (Kabsch, 1993).

2.5. Structure determination and refinement

The structure of LATA was solved by the molecular-replacement method with *MOLREP* (Vagin & Teplyakov, 2010) in the *CCP*4 suite (Winn *et al.*, 2011) using the structure of low-specificity L-*allo*-threonine aldolase from *Thermotoga maritima* (tm1744; PDB entry 2fm1; 51% sequence identity; Joint Center for Structural Genomics, unpublished work) as a search model. Manual model building and refinement were performed with *Coot* (Emsley *et al.*, 2010) and *REFMAC*5 (Murshudov *et al.*, 2011), respectively. The structure of LATA_H128Y/S292R was determined by the molecular-replacement method using the structure of LATA as the initial model. We did not use a data cutoff during refinement.

We failed to obtain any crystals of the complex of LATA with L-*allo*-threonine after extensive efforts including co-crystallization and soaking experiments. L-*allo*-Threonine was docked into the LATA structure based on the superposition of *T. maritima* threonine aldolase (TMTA; PDB entry 1m6s; Kielkopf & Burley, 2002) and *E. coli* threonine aldolase (eTA; PDB entry 4lnl; di Salvo *et al.*, 2014). The D-*allo*-threonine molecule was generated using the *PRODRG* server (Schüttelkopf & van Aalten, 2004). The model was docked into the crystal structure of LATA using *PyMOL* (http://www.pymol.org) and then superimposed on L-*allo*-threonine.

Table 1
Data-collection and refinement statistics.

Values in parentheses are for the highest resolution shell.

	LATA	LATA_H128Y/S292R
Data collection		
Beamline	AR-NW12A, PF	AR-NW12A, PF
Wavelength (Å)	1.00000	1.00000
Space group	$P2_1$	$P2_1$
Unit-cell parameters (Å, °)	a = 82.5, b = 95.9, c = 94.9, β = 113.6	a = 78.8, b = 93.4, c = 94.0, β = 113.9
Resolution (Å)	50.0–2.59 (2.63–2.59)	50.0–2.50 (2.56–2.50)
No. of unique reflections	41738	42773
Multiplicity	3.5	3.7
Completeness (%)	99.3 (99.5)	98.8 (98.5)
R_{merge}†	0.070 (0.160)	0.073 (0.270)
$\langle I/\sigma(I)\rangle$	30.3 (10.7)	15.6 (5.2)
Refinement		
Resolution limits (Å)	50.0–2.60 (2.67–2.60)	46.7–2.50 (2.56–2.50)
Sigma cutoff (F)	0	0
No. of reflections	39376 (2920)	42715 (2647)
R_{work} (%)	23.3 (26.0)	18.6 (21.9)
R_{free}‡ (%)	28.3 (33.4)	24.7 (32.9)
R.m.s.d.§		
Bond lengths (Å)	0.006	0.003
Bond angles (°)	1.04	0.84
No. of atoms		
Protein	9797	9755
Ligand	85	80
Water	169	363
Average B factor (Å^2)		
Protein	22.9	29.8
Ligand	21.4	28.4
Water	13.8	26.7
Ramachandran analysis¶		
Favoured (%)	97.5	98.4
Allowed (%)	2.5	1.6
Outliers (%)	0	0

† $R_{merge} = \sum_{hkl}\sum_i |I_i(hkl) - \langle I(hkl)\rangle| / \sum_{hkl}\sum_i I_i(hkl)$, where $I_i(hkl)$ is the ith intensity measurement of the reflection hkl, including symmetry-related reflections, and $\langle I(hkl)\rangle$ is its average. ‡ R_{free} was calculated with 5% of reflections that were excluded from refinement. § Root-mean-square deviation. ¶ Calculated by *MolProbity*.

2.6. Activity assay for purified enzymes

The measurements of LATA activity were performed as reported previously (Liu, Dairi *et al.*, 1997). In brief, the protein solution was incubated with L-*allo*-threonine or L-threonine as a substrate at 303 K, and the released acetaldehyde was measured spectrophotometrically by coupling the reduction of acetaldehyde (oxidation of NADH) with yeast alcohol dehydrogenase (Wako Pure Chemical Industries). The reaction mixture comprised 100 µmol Tris–HCl buffer pH 8.0, 0.2 µmol NADH, 30 U yeast alcohol dehydrogenase, 0.05 µmol PLP, 8 µmol substrate and appropriate amounts of the enzyme in a final volume of 1 ml. One unit of aldolase activity was defined as the amount of enzyme that catalyzes the formation of 1 µmol of acetaldehyde (1 µmol of NADH oxidized) per minute at 303 K. The measurements of the threonine aldolase activity of eTA, LTAS from *Saccharomyces cerevisiae* and LTAP from *Pseudomonas* sp. were also

performed as reported previously (Liu, Nagata *et al.*, 1997; Liu, Dairi *et al.*, 1998; Liu, Ito *et al.*, 1998).

3. Results and discussion

3.1. Random mutagenesis

Random mutagenesis was performed in a 1060 bp DNA region encoding the entire 1017 bp LATA ORF, as described in §2. The conditions used for error-prone PCR were based on a desired substitution frequency of one to three substitutions per 1000 bp. In the screening of the mutant enzymes, approximately 3000 clones were screened for activity towards L-*allo*-threonine and L-threonine. Among them, only one variant showed significant activity towards not only L-*allo*-threonine but also L-threonine. From the sequencing results, three base substitutions were observed in the mutant gene: C382T, T765C and T876A. The T765C mutation was a silent mutation and therefore the mutant enzyme had two amino-acid substitutions H128Y and S292R. To clarify the contribution of each substitution to the stereoselectivity, plasmids encoding the single-mutant enzymes H128Y and S292R were constructed as described in §2.

3.2. Overall structures of LATA and its mutant

The crystal structures of LATA and LATA_H128Y/S292R were determined at 2.59 and 2.50 Å resolution, respectively. The crystallographic R_{work} and R_{free} factors were 23.5 and 28.3%, respectively, for LATA and 19.3 and 24.2%, respectively, for LATA_H128Y/S292R. The asymmetric units of the LATA crystals and the mutant crystals contained four LATA protomers and four PLP–glycine complex (PLP-Gly) molecules. Most of the residues of LATA and LATA_H128Y/

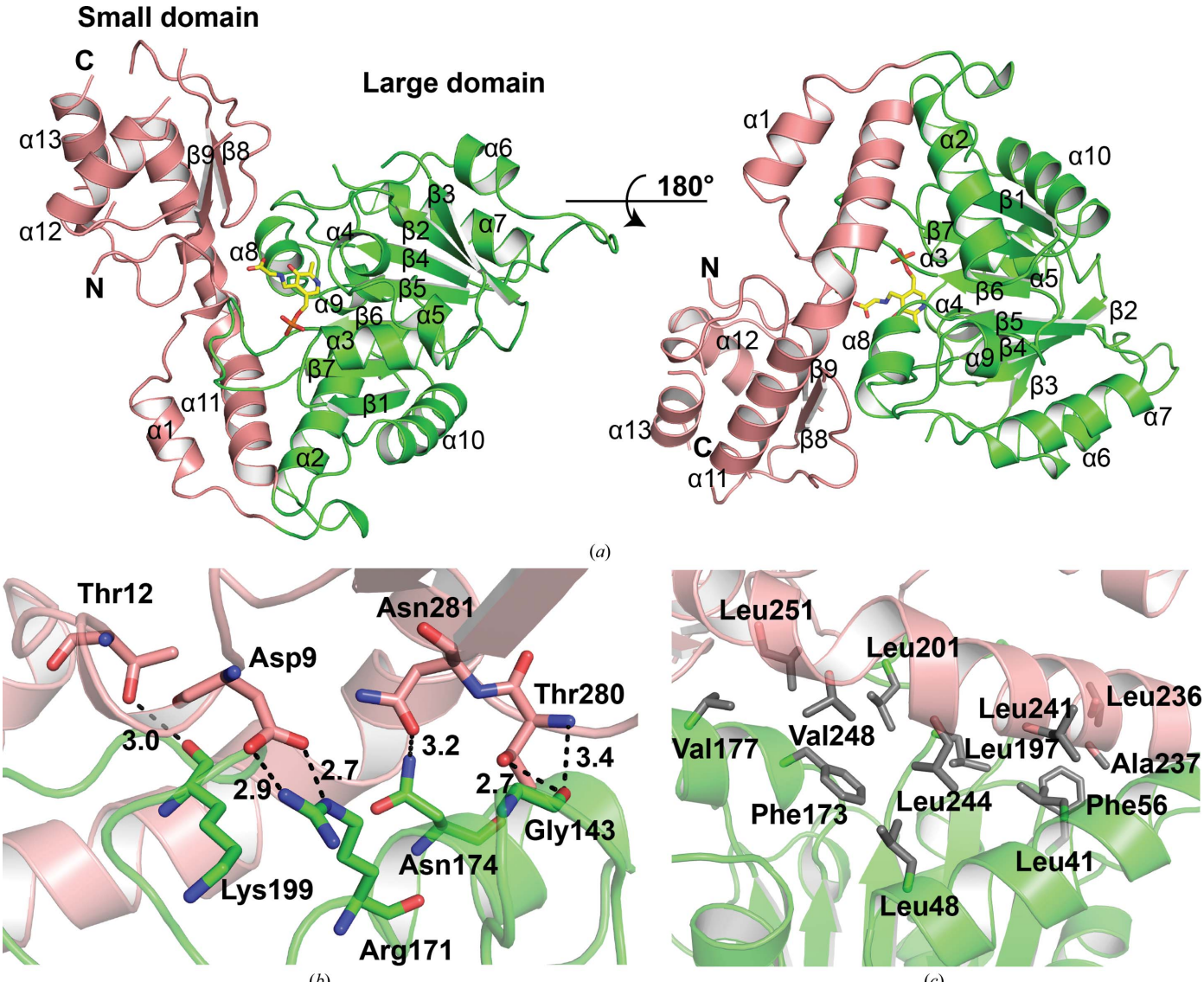

Figure 1
(*a*) Ribbon representation of the LATA protomer structure. The small domain and the large domain are shown in salmon and green, respectively. PLP-Gly is shown as yellow sticks. The interdomain hydrogen bonds/salt bridges (*b*) and hydrophobic interactions (*c*) formed between the two domains are also shown.

S292R (97.5 and 98.2%, respectively) are in the most favoured region of the Ramachandran plot. The data-collection and refinement statistics are summarized in Table 1.

The structure of LATA contained 13 α-helices and nine β-strands and possessed two α/β domains (Fig. 1*a*). The large domain consisted of a central seven-stranded parallel β-sheet ($\beta1$–$\beta7$) flanked by nine α-helices ($\alpha2$–$\alpha10$) on both sides. The small domain was comprised of two β-strands ($\beta8$ and $\beta9$) and four α-helices ($\alpha1$ and $\alpha11$–$\alpha13$) at the periphery. The two domains within each protomer formed several interdomain hydrogen bonds/salt bridges (Fig. 1*b*): Thr12 OG1–Lys199 O (3.0 Å), Asp9 OD1–Arg171 NH2 (2.9 Å), Asp9 OD2–Arg171 NE (2.7 Å), Asn281 OD1–Asn174 ND2 (3.2 Å), Thr280 OG1–Gly143 O (2.7 Å) and Thr280 N–Gly143 O (3.4 Å). Hydrophobic interactions were also formed by the side chains of Leu41, Leu48, Phe56, Val177, Leu197, Leu201 and Phe173 in the large domain with Leu236, Ala237, Leu241, Val248, Leu244 and Leu251 in the small domain (Fig. 1*c*).

The threonine aldolase family members have been reported to function as tetramers (Liu, Dairi *et al.*, 1997; Kielkopf & Burley, 2002). In the structure of LATA (Fig. 2*a*), chains *A* and *B* or chains *C* and *D* form intimate 'catalytic dimer' interfaces between the two large domains. The interface of the catalytic dimer was calculated to have a buried surface area of 1863 Å^2 per protomer by the *PISA* server (Krissinel & Henrick, 2007), which corresponded to 13.3% of the protomer surface. The two protomers of chains *A* and *B* formed salt bridges and hydrogen bonds between each other, *i.e.* Arg7 NH1/2–Glu34 OE1/2 (2.6 and 2.8 Å), Thr10 OG1–Asp29 OD2 (2.7 Å), Gln13 NE2–Val27 O (2.8 Å), Ser59 OG–Gly227 O (2.7 Å), Arg19 NH1–Leu23 O (2.8 Å), Arg19 NH1/2–Ala25 O (2.9 and 3.1 Å), Gln232 NE2–Thr10 O (3.1 Å), Gln232 N–Pro204 O (2.8 Å) and Arg231 NH1–Thr10 OG1 (3.2 Å) (Fig. 2*b*). These interactions serve as key structural features in stabilizing the three-dimensional quaternary structure.

On the other hand, the overall structure of LATA is similar to that of LATA_H128Y/S292R, with a root-mean-square deviation (r.m.s.d.) of 0.2 Å for 263 C$^\alpha$ atoms of chain *A* between the two structures. The significant structural changes occurred in the residues between Ala123 and Pro131 (Fig. 3),

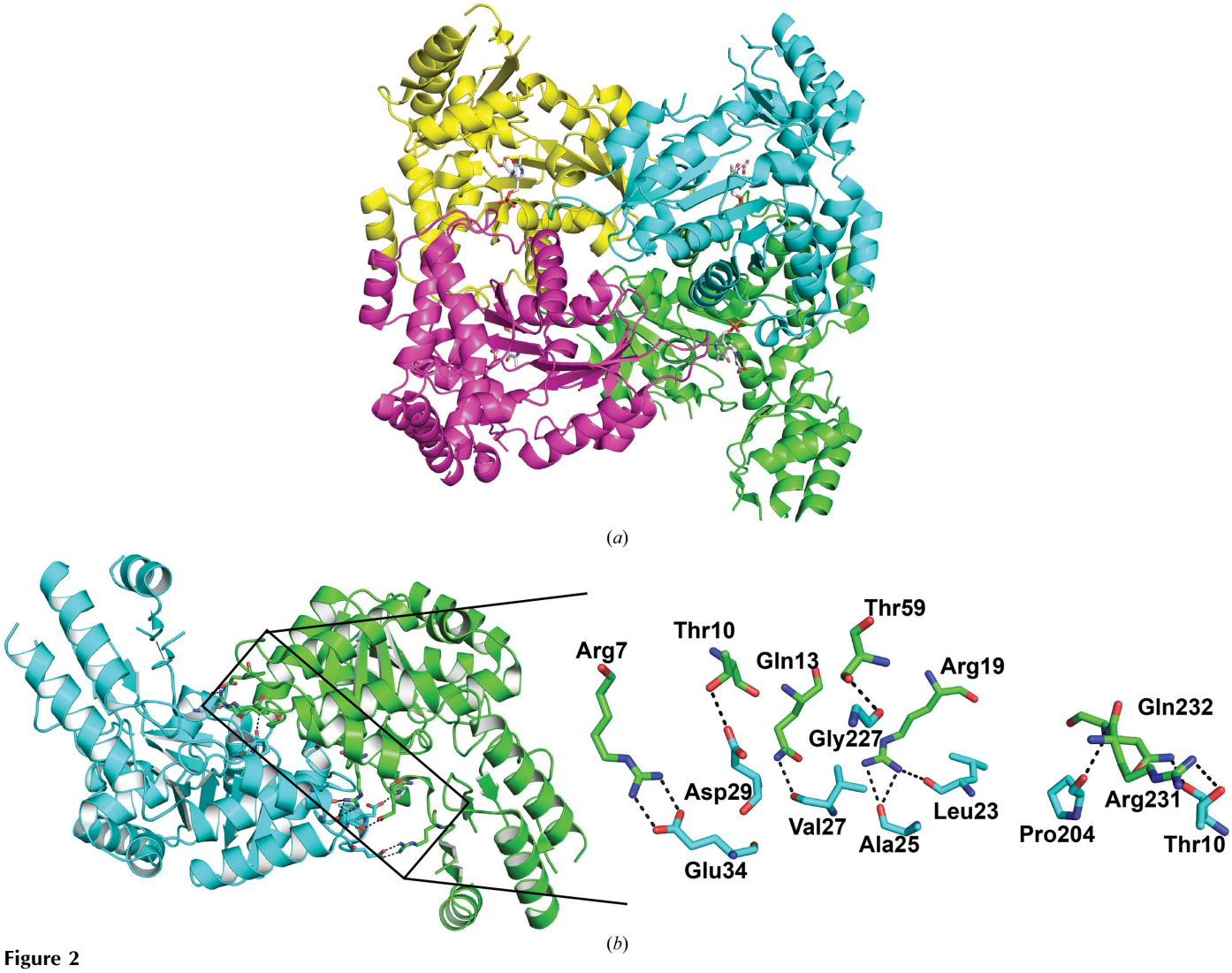

(*a*)

(*b*)

Figure 2
(*a*) Ribbon representation of LATA in an asymmetric unit. The four protomers are coloured cyan (chain *A*), green (chain *B*), magenta (chain *C*) and yellow (chain *D*). (*b*) Hydrogen bonds/salt bridges are shown as sticks in the dimeric structure.

Table 2
Kinetic parameters for the activity of LATA and its mutants towards L-*allo*-threonine and L-threonine.

	L-*allo*-Thr			L-Thr		
Enzyme	k_{cat} (s^{-1})	K_m (mM)	k_{cat}/K_m (mM^{-1} s^{-1})	k_{cat} (s^{-1})	K_m (mM)	k_{cat}/K_m (mM^{-1} s^{-1})
LATA	13.8	0.513	26.9	0.641	31.6	0.00203
H128Y/S292R	22.0	0.386	83.3	2.14	3.27	0.654
H128Y	16.5	0.402	41.0	1.81	4.48	0.404
S292R	18.3	0.444	41.2	0.913	32.7	0.0279

where His128 moved 4.2 Å when it was mutated to Tyr. His128 has been reported to function as a catalytic base (Kielkopf & Burley, 2002; di Salvo *et al.*, 2014). The hydroxyl group of Tyr128 forms a hydrogen bond to the carbonyl group of Val31. The large displacement of His128 in the mutation to a Tyr residue would not arise from a crystal-packing artifact (Supplementary Fig. S3*a*). The significance of H128Y regulating the substrate stereoselectivity will be discussed later. We could not find the residues Ser292 in the wild type and Arg292 in the H128Y/S292R mutant in the electron-density maps. We could not, therefore, confirm how Ser292 in the wild-type enzyme and Arg292 in the H128Y/S292R mutant differ.

3.3. Binding mode of PLP-Gly in the active site

LATA binds PLP-Gly in the cavity of the active site, in which the phosphate group and the external aldimine of PLP-Gly are located, at positively charged residues (Fig. 4*a*). PLP-Gly binds to residues Ser8, Lys199 and Arg313 of the small domain and Gly60, Thr61, His85, Asp168 and Arg171 of the large domain (Fig. 4*b* and Supplementary Fig. S4). In addition, Arg231 from the neighbouring chain is located at the active site and binds to the phosphate group of PLP-Gly. The aldimine interacts with the side chains of Arg171, Arg313 and Ser8, which are considered to anchor the substrate/product to the active site. Arg171 provides a second positive charge to stabilize the substrate/product and intermediate resonance states along the reaction pathway *via* interactions with the carboxylate. PLP N1 and PLP O3 interact with Asp168 and Arg171, respectively. The imidazole ring of His85 stacks with the pyridine ring of PLP-Gly and has been reported to regulate the degree of stereospecificity of threonine aldolases for L-*allo*-threonine *versus* L-threonine (di Salvo *et al.*, 2014; Kielkopf & Burley, 2002). In the threonine aldolase family, most of the active-site residues that recognize substrate/product are conserved, including Ser8, His85, Arg171, Lys199 and Arg313. In the active site, the Lys199 responsible for Schiff-base formation with PLP is conserved in this family of enzymes (Liu, Dairi *et al.*, 1997; Kielkopf & Burley, 2002). The glycine ligand is bound in an orientation that resembles the ternary complex, with its amino groups slightly out of the plane of the PLP-Gly ring, and the scissile bond of the aldimine is oriented perpendicular to the plane of the PLP-Gly ring.

3.4. Comparison of LATA and its mutant with other aldolases

LATA catalyzes the reversible interconversion of L-*allo*-threonine in preference to that of L-threonine: the k_{cat}/K_m values of LATA were 26.9 mM^{-1} s^{-1} towards L-*allo*-threonine and only 0.00203 mM^{-1} s^{-1} towards L-threonine (Table 2). However, LATA_H128Y/S292R showed threefold and 322-fold increased k_{cat}/K_m values towards these two substrates compared with the wild-type enzyme. It is notable that the H128Y and the S292R mutants showed similar k_{cat}/K_m values toward L-*allo*-threonine, while the H128Y mutant showed a higher value towards L-threonine than the S292R mutant, suggesting that the improved activity was likely to be caused by the mutation of His128 to Tyr. The improved activity of S292R towards L-*allo*-threonine and L-threonine could not be explained from the structural information because the loops between β8 and α12 including Ser292 or S292R in LATA and its mutant are disordered.

Structural alignment using the *DALI* server (Holm & Sander, 1995) showed that the overall structure of LATA is highly similar to those of previously reported enzymes, including TMTA with 49% identity (*Z*-score 47.9; r.m.s.d. 1.2 Å) and eTA with 54% identity (*Z*-score 48.3; r.m.s.d. 1.0 Å). Structural superposition of LATA and its mutant with TMTA and eTA reveals that the $C^{\alpha}-C^{\beta}$ bond of L-*allo*-threonine, which is perpendicular to the plane of the PLP-Gly ring, may allow the enzyme to take advantage of stereoelectronic effects during catalysis (Dunathan, 1971; Kielkopf & Burley, 2002). The substrate-binding model is consistent with the activity assay (Fig. 5 and Table 2). Based on the superposed structures, the hydroxyl group of L-*allo*-threonine is recognized by the side chains of His85 and His128 (Fig. 5*a*). These two residues are conserved in the threonine aldolase family. The interaction between the side chains of these two histidines and the hydroxyl group of L-*allo*-threonine would explain the preferable substrate stereoselectivity

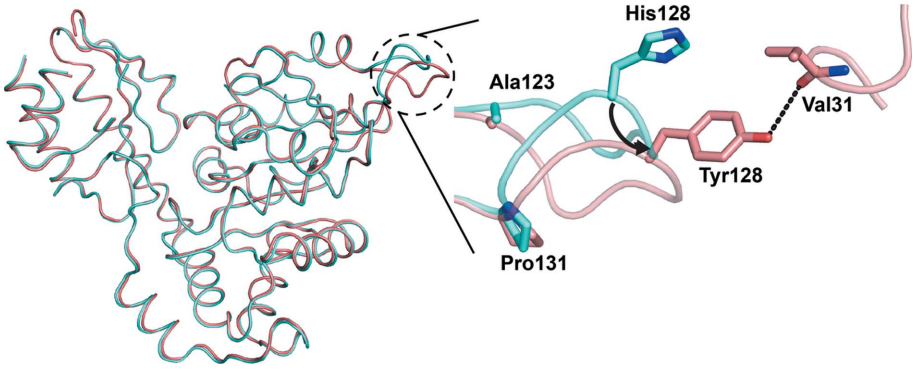

Figure 3
Superposition of the structures of LATA (cyan) and LATA_H128Y/S291R (salmon). The different conformation in these two protomers is indicated by a dashed circle. The residues His128 and H128Y are indicated with cyan and salmon sticks, respectively.

towards L-*allo*-threonine. Two residues, Glu90 and Asp126, which are located in the hydrogen-bonding network of the active site, were observed to play important roles in aiding two histidines (His85 and His128) during the recognition of substrates (Fig. 5*a* and Supplementary Table S1). The E90A mutant in particular showed extremely low activity towards the two substrates, suggesting that Glu90 assists His85 in removing the proton from the L-*allo*-threonine hydroxyl group. The D126A mutation changed the substrate selectivity like the H128Y mutation, which suggests that Asp126 supports His128 in recognizing L-*allo*-threonine in preference to L-threonine in the wild-type enzyme.

On the other hand, the methyl group of L-*allo*-threonine could be recognized *via* a CH_3–π interaction with the benzene ring of Tyr89. TMTA has a tyrosine residue at the same position, while eTA has a phenylalanine residue. Comparing the unliganded and substrate-complex structures, the side chains of Tyr87 in TMTA and Phe87 in eTA showed an almost identical spatial orientation (Supplementary Fig. S5). Therefore, we presume that the side chains of Tyr89 in the LATA substrate-binding model may also retain a similar spatial orientation as in the PLP-Gly binding structure. Superposition

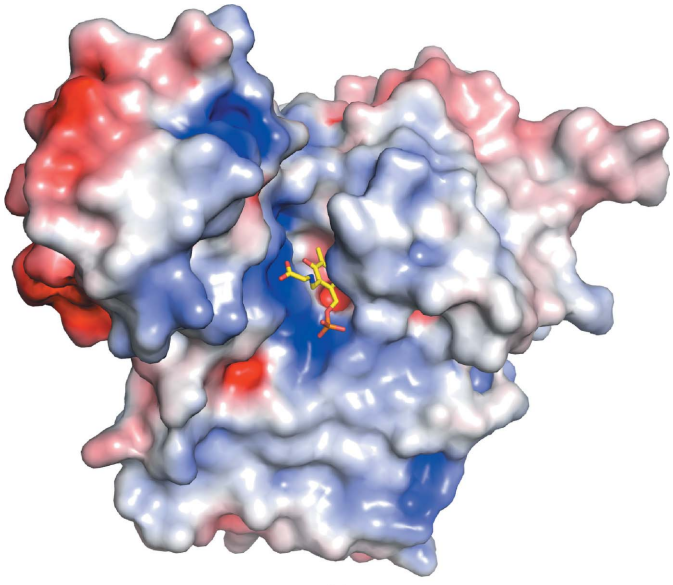

(*a*)

(*b*)

Figure 4
Overview of the active site in the LATA–PLP-Gly structure. (*a*) Electrostatic surface potential displayed in blue for positive ($5kTe^{-1}$), red for negative ($-5kTe^{-1}$) and white for neutral. PLP-Gly is indicated with yellow sticks. (*b*) Interaction between PLP-Gly (yellow) and the LATA protein. Dotted lines show potential hydrogen bonds. The loop in magenta is from the other protomer in the dimer.

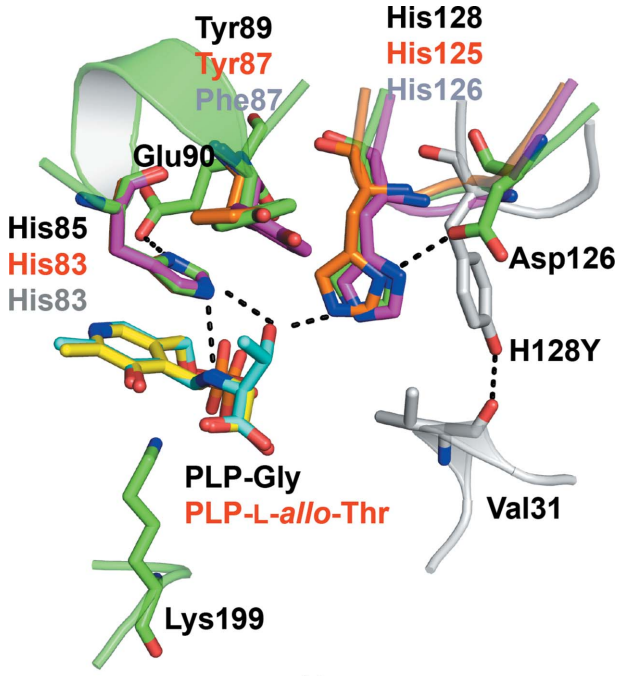

(*a*)

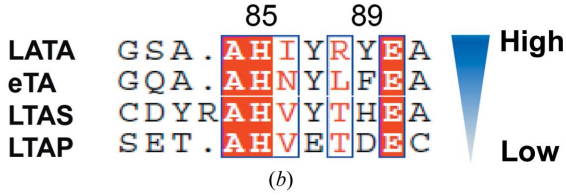

(*b*)

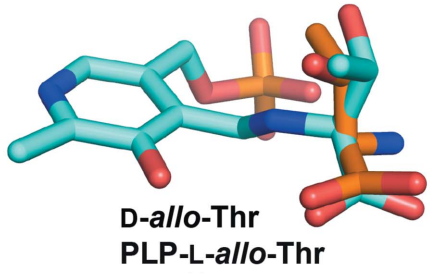

(*c*)

Figure 5
(*a*) Superposition of the active sites of LATA (green), LATA_H128Y/S291R (white), TMTA (PDB entry 1lw4; magenta) and eTA (PDB entry 4lnm; orange); the catalytic residues are labelled in black for LATA and its mutant, red for TMTA and grey for eTA. Dashed lines indicate hydrogen bonds. (*b*) Sequence alignment of L-threonine aldolases from *Aeromonas jandaei* (LATA), *Escherichia coli* (eTA), *Saccharomyces cerevisiae* (LTAS) and *Pseudomonas* sp. (LTAP). (*c*) Superposition of PLP–L-*allo*-Thr (cyan) and D-*allo*-threonine (orange).

Table 3
The relative activity of threonine aldolases from different organisms towards L-*allo*-threonine and L-threonine.

The activity of wild-type LATA towards each substrate is represented as 100. The cell-free extracted threonine aldolases were prepared and 8 m*M* substrate was added to the reaction mixture.

	Relative activity (%)		
Enzyme	L-*allo*-Thr	L-Thr	Specificity ratio L-*allo*-Thr/L-Thr
LATA	100	100	47.4
eTA	18.3	189	4.60
LTAS	3.70	379	1.93
LTAP	36.8	1719	1.02

of LATA with TMTA and eTA showed that the spatial orientation of the benzene ring of Tyr89 (LATA) was different from that of Tyr89 (TMTA) and Phe87 (eTA) (Fig. 5*a*). These differences may partly explain the reason why LATA has an extremely high selectivity towards L-*allo*-threonine. Sequence alignment showed that Phe87 was also not conserved in other threonine aldolases (Fig. 5*b*). The activity assay of LATA, eTA, LTAS and LTAP revealed that the Tyr, Phe or His contributes to discriminating L-*allo*-threonine from L-threonine (Table 3), which further supports that the stereoselectivity toward L-*allo*-threonine requires an interaction between the methyl group of L-*allo*-threonine and the benzene ring. Furthermore, LATA showed no activity towards D-*allo*-threonine because it could not form the intermediate with PLP (Fig. 5*c*).

A structural comparison between LATA and LATA_H128Y/S292R reveals a structural change of residues Ala123–Pro131 (Fig. 3), where His128 of the third protomer in the tetrameric complex is located in the active site. However, His128 moves 4.2 Å outwards from the active site on mutation to Tyr, which changes the degree of substrate stereoselectivity for L-*allo*-threonine *versus* L-threonine. In the LATA_H128Y/S292R structure, a new hydrogen bond between the hydroxyl group of Tyr128 and the carbonyl group of Val31 replaced the original hydrogen bond between the L-*allo*-threonine OG1 atom and His128 of wild-type LATA (Fig. 5*a*). An alignment comparison of wild-type LATA with TMTA and eTA revealed that the loop Ala123–Pro131 showed a slightly different spatial orientation (Supplementary Fig. S3*b* and Fig. 5*a*). It is obvious that the H128Y mutation caused the conformational changes. This observation explains why the mutation to Tyr128 causes broad substrate stereoselectivity (Supplementary Table S2).

To confirm that His128 regulates the stereoselectivity of LATA towards L-*allo*-threonine and L-threonine, we carried out saturation mutagenesis of His128. The results revealed that substitution by only a few amino acids, *i.e.* Tyr, Phe and Met, resulted in a higher activity towards L-*allo*-threonine than was shown by wild-type LATA (Supplementary Table S2). However, substitution by Tyr, Phe, Leu, Ser, Met, Trp, Ile, Lys and Val yielded a higher activity towards L-threonine than in the wild-type enzyme. The H128Y mutant showed the highest activity towards the two substrates (8.4-fold towards L-threonine and 2.0-fold towards L-*allo*-threonine compared with the wild-type enzyme). Most substitutions by hydrophobic residues improved the activity towards L-threonine. This was considered to show that the hydrophobic interaction between the methyl group of L-threonine and the side chains of the mutated hydrophobic residues caused the LATA mutants to preferably catalyze interconversion of L-threonine compared with L-*allo*-threonine. It is noteworthy that the H128D mutant showed a high specificity ratio for L-*allo*-threonine/L-threonine (136:1). This suggested strengthened stereoselective recognition towards L-*allo*-threonine, although this mutant exhibited low activity towards the two substrates.

4. Conclusions

We determined the crystal structures of LATA and its H128Y/S292R mutant. Their superposed structures implied that conformational changes take place in the loop consisting of the residues between Ala123 and Pro131, where the residue His128 moved 4.2 Å outwards from the active site on mutation to Tyr. His85 and His128 were located near the OG1 atom of L-*allo*-threonine at the active site. Furthermore, the saturation mutagenesis of His128 was consistent with the substrate-binding model in showing that His128 together with His85 and Tyr89 plays an important role in the substrate specificity. Our work on LATA and its mutants of the His128 residue provides further insights into the regulation of the substrate stereoselectivity of threonine aldolases towards L-*allo*-threonine/L-threonine.

This work was supported by the National Project on Targeted Proteins Research Program and the Platform for Drug Design, Discovery and Development from the Ministry of Education, Culture, Sports, Science and Technology, Japan. We would like to thank the scientists and staff at the Photon Factory. The synchrotron-radiation experiments were performed on the AR-NW12A beamline at the Photon Factory, Tsukuba, Japan (Proposal No. 2008S2-001).

References

di Salvo, M. L., Remesh, S. G., Vivoli, M., Ghatge, M. S., Paiardini, A., D'Aguanno, S., Safo, M. K. & Contestabile, R. (2014). *FEBS J.* **281**, 129–145.
Dunathan, H. C. (1971). *Adv. Enzymol. Relat. Areas Mol. Biol.* **35**, 79–134.
Emsley, P., Lohkamp, B., Scott, W. G. & Cowtan, K. (2010). *Acta Cryst.* D**66**, 486–501.
Gwon, H. J. & Baik, S. H. (2010). *Biotechnol. Lett.* **32**, 143–149.
Holm, L. & Sander, C. (1995). *Trends Biochem. Sci.* **20**, 478–480.
Kabsch, W. (1993). *J. Appl. Cryst.* **26**, 795–800.
Karasek, M. A. & Greenberg, D. M. (1957). *J. Biol. Chem.* **227**, 191–205.
Kielkopf, C. L. & Burley, S. K. (2002). *Biochemistry*, **41**, 11711–11720.
Krissinel, E. & Henrick, K. (2007). *J. Mol. Biol.* **372**, 774–797.
Kumagai, H., Nagate, T., Yoshida, H. & Yamada, H. (1972). *Biochim. Biophys. Acta*, **258**, 779–790.
Liu, J.-Q., Dairi, T., Itoh, N., Kataoka, M., Shimizu, S. & Yamada, H. (1998). *Eur. J. Biochem.* **255**, 220–226.
Liu, J.-Q., Dairi, T., Kataoka, M., Shimizu, S. & Yamada, H. (1997). *J. Bacteriol.* **179**, 3555–3560.

Liu, J.-Q., Ito, S., Dairi, T., Itoh, N., Kataoka, M., Shimizu, S. & Yamada, H. (1998). *Appl. Environ. Microbiol.* **64**, 549–554.
Liu, J.-Q., Nagata, S., Dairi, T., Misono, H., Shimizu, S. & Yamada, H. (1997). *Eur. J. Biochem.* **245**, 289–293.
Matsuda, T., Yamanaka, R. & Nakamura, K. (2009). *Tetrahedron Asymmetry*, **20**, 513–557.
Matthews, R. G., Drummond, J. T. & Webb, H. K. (1998). *Adv. Enzyme Regul.* **38**, 377–392.
Murshudov, G. N., Skubák, P., Lebedev, A. A., Pannu, N. S., Steiner, R. A., Nicholls, R. A., Winn, M. D., Long, F. & Vagin, A. A. (2011). *Acta Cryst.* D**67**, 355–367.
Ogawa, H., Gomi, T. & Fujioka, M. (2000). *Int. J. Biochem. Cell Biol.* **32**, 289–301.
Otwinowski, Z. & Minor, W. (1997). *Methods Enzymol.* **276**, 307–326.
Patel, R. N. (2008). *Coord. Chem. Rev.* **252**, 659–701.
Roberto, P., Roberto, L., Lucia, T., John, C., Maria, P. & Enrico, M. (1991). *Biochem. Soc. Trans.* **19**, 346S–347S.
Savile, C. K., Janey, J. M., Mundorff, E. C., Moore, J. C., Tam, S., Jarvis, W. R., Colbeck, J. C., Krebber, A., Fleitz, F. J., Brands, J., Devine, P. N., Huisman, G. W. & Hughes, G. J. (2010). *Science*, **329**, 305–309.
Schirch, L. & Gross, T. (1968). *J. Biol. Chem.* **243**, 5651–5655.
Schüttelkopf, A. W. & van Aalten, D. M. F. (2004). *Acta Cryst.* D**60**, 1355–1363.
Shibata, K., Shingu, K., Vassiley, V. P., Nishide, K., Fujita, T., Node, M., Kajimoto, T. & Wong, C.-H. (1996). *Tetrahedron Lett.* **37**, 2791–2794.
Vagin, A. & Teplyakov, A. (2010). *Acta Cryst.* D**66**, 22–25.
Vassilev, V. P., Uchiyama, T., Kajimoto, T. & Wong, C.-H. (1995). *Tetrahedron Lett.* **36**, 5063–5064.
Winn, M. D. *et al.* (2011). *Acta Cryst.* D**67**, 235–242.